One-dimensional model for microemulsions

M. W. Matsen and D. E. Sullivan
Department of Physics and Guelph-Waterloo Program for Graduate Work in Physics, University of Guelph, Guelph, Ontario, Canada N1G 2W1
(Received 11 April 1991)

In this paper, a model for water-oil-surfactant mixtures, which we have previously studied on two- and three-dimensional lattices, is now studied on a one-dimensional lattice. In this case we are able to obtain exact results, whereas on the higher-dimensional lattices it was necessary to use approximations. This one-dimensional model produces correlation and structure functions that are similar to those obtained for the disordered phase on the two- and three-dimensional lattices. The disorder line is obtained from the water-water correlation function and the Lifshitz line is derived from the water-water structure function. One or the other of these lines is typically used to divide the disordered phase into a region of ordinary disordered fluid and a microemulsion region. Both these lines calculated exactly for the one-dimensional lattice behave similarly to their counterparts on the two- and three-dimensional lattices calculated by various approximations.

I. INTRODUCTION

Water-oil-surfactant mixtures can exist as microemulsions because of the strong tendency of surfactant molecules to be adsorbed at water-oil interfaces. In this case, the water and oil are mixed down to microscopic scales whereas without the surfactant they would phase separate [1]. A microemulsion with considerably more water than oil consists of small spheres of oil surrounded by a surfactant monolayer and randomly dispersed in the water. The reverse happens when there is considerably more oil than water. When the water and oil concentrations are comparable, as considered in this paper, the water and oil form bicontinuous interweaving tubelike structures where a surfactant monolayer exists on the vast interface between water and oil. Although these bicontinuous structures are formed from tubes with microscopic sized cross sections, they form a network that spans macroscopic distances.

The microemulsion does not have any rigid structure or long-range order and thus appears as a uniform disordered phase [1–9]. In order to characterize the microemulsion phase by methods of statistical mechanics, one examines the correlation and structure functions. For example, the average diameter of the tubes making up the bicontinuous structure for water causes an oscillation in the water-water correlation function of comparable wavelength. This oscillation in the water-water correlation function can cause a peak in the water-water structure function at small nonzero wave vectors. Increasing the surfactant concentration presumably creates finer bicontinuous structures with more surface area, which decreases the wavelength of the oscillation in the water-water correlation function and moves the peak in the water-water structure function to larger wave vectors. Part of our aim is to reproduce this behavior in the correlation and structure functions.

In recent years, much effort has gone into modeling water-oil-surfactant mixtures [1–14] and other similar systems [15,16]. Rather than attempting to examine realistic models, the focus has been on producing simple models that hopefully still retain the essential features of these mixtures. These simple models usually employ a lattice [1–8,10–12] rather than allowing molecules the freedom to occupy any point in space [12,13]. In most cases, as in the present work, each lattice site is occupied by either water, oil, or surfactant. The justification for examining these lattice models is that they can be tackled by numerous statistical approaches. By using a lattice model, more accurate approximations and sometimes, as in the case here, exact solutions are possible. Also these models generally have fewer parameters, making it much easier to determine the effects of each parameter on the model.

In this paper we consider a model on a one-dimensional lattice, which was first introduced in Ref. [2] and studied there on a more realistic three-dimensional lattice. The strongest justification for considering the model on a one-dimensional lattice is that it can be solved exactly by the transfer-matrix method [3]. The main drawback with one-dimensional models is that they generally do not exhibit phase transitions except at zero temperature. Instead, they may have different regions with distinct characteristics but without the well-defined phase boundaries present in higher-dimensional lattices. Hence aspects such as phase diagrams and surface tensions, both important in the study of water-oil-surfactant mixtures, cannot be properly considered. Nevertheless, we find that correlation and structure functions for the present model [2] do seem to have the same behavior on the one-dimensional lattice as on higher-dimensional lattices. Therefore, our main focus will be on these two functions which are of importance in microemulsions. It turns out that the bicontinuous structure of a microemulsion, present when the water and oil concentrations are similar, is not possible in either one or two dimensions [1,17], but it is not explicitly the bicontinuous structure of the microemulsion that affects the behavior of the correlation

and structure functions. If one was considering the electrical conductivity of the microemulsion, its bicontinuous structure would be important.

We are aware of two papers that examine similar one-dimensional lattice models. The first, by Gompper and Schick [3], is also solved exactly by the transfer-matrix method, but has significantly different interactions from those considered here. In particular, that model [3-5] does not include orientational degrees of freedom for the surfactant molecules but rather uses a three-particle interaction that favors having water and oil on opposite sides of a surfactant molecule. The second model on the one-dimensional lattice, considered by Ciach [6], is slightly less general than the present model. As well, it is not solved exactly but rather by a mean-field approximation, which artificially creates phase transitions. To calculate results, in terms of the parameters used in Ref. [6] from formulas present in this paper, set $J_1=b$, $J_2=c$, $J_3=0$, $K_1=0$, $K_2=0$, and $K_3=0$. (The J_i's and K_i's will be defined in Sec. II.)

II. THE MODEL

On the one-dimensional lattice, each lattice site will have four possible states, water, oil, and two orientations of surfactant. The lattice sites are labeled sequentially from 1 to N, where N is the total number of lattice sites. For the i^{th} lattice site, there is a state variable x_i which takes on the values 1, 2, 3, and 4 when the site is occupied by water, oil, surfactant pointing to the right, and surfactant pointing to the left, respectively. Unlike the model in Ref. [2], the unnecessary orientational degrees of freedom for the water and oil are not explicitly included.

The Hamiltonian described in Ref. [2] for the three-dimensional lattice, on the above one-dimensional lattice becomes

$$H=\sum_{i=1}^{N}\left[V_2(x_i,x_{i+1})+V_1(x_i)\right], \tag{1}$$

where V_2 and V_1 are the two and one-particle potentials, respectively. $V_2(a,b)$ is given in Table I and $V_1(a)=0$, 0, $-\mu_S$, and $-\mu_S$ for $a=1,2,3$, and 4, where μ_S is the surfactant chemical potential. The variable x_{N+1} is defined to equal x_1 so that in fact we are imposing periodic boundary conditions. This boundary condition is used only because it is most convenient. We will always give results in the thermodynamic limit where $N\to\infty$, and the actual boundary conditions are immaterial.

The Hamiltonian has a "spin-reversal" symmetry described in Ref. [2], where it is invariant under a simultaneous interchange of water with oil (i.e., $x_i=1\leftrightarrow x_i=2$ for all i) and of surfactant orientation (i.e., $3\leftrightarrow 4$). Although it is realized that such symmetries are not valid in real water-oil-surfactant mixtures, they are often used because they greatly simplify a model while retaining the essential elements of the ternary mixture [6]. In this particular case, it means there are only six distinct bonds, which are shown in Table II. (An open circle represents water, a closed circle represents oil. The arrow, which represents a surfactant molecule, points in the direction of the polar head group.)

TABLE I. The two-particle potential $V_2(a,b)$ of the present model.

a \ b	1	2	3	4
1	$-J_1-K_1$	J_1-K_1	J_2-K_2	$-J_2-K_2$
2	J_1-K_1	$-J_1-K_1$	$-J_2-K_2$	J_2-K_2
3	$-J_2-K_2$	J_2-K_2	J_3-K_3	$-J_3-K_3$
4	J_2-K_2	$-J_2-K_2$	$-J_3-K_3$	J_3-K_3

While there are six parameters used to specify the six distinct bonds in Table II, not all of these six parameters are necessary. This is because the substitutions $K_1\Longrightarrow K_1+\Delta_1$, $K_2\Longrightarrow K_2+\Delta_1$ and $K_3\Longrightarrow K_3+\Delta_1$ simply change the total energy of all states by the constant amount $-N\Delta_1$, which does not affect the statistics of the model. Thus by choosing Δ_1 appropriately any one of the K_i's can always be set to zero without loss of generality. It is possible to set one other K_i to zero without loss of generality, because the substitutions $K_2\Longrightarrow K_2+\Delta_2$, $K_3\Longrightarrow K_3+2\Delta_2$ and $\mu_S\Longrightarrow\mu_S-2\Delta_2$ do not change the energy of a state for any value Δ_2. Nevertheless, all six parameters are retained in future calculations as there is no significant simplification by not doing so.

The lattice spacing has been used to define a distance scale and now the parameter J_1 will be used to set an energy scale. More specifically, energy will be measured in units of J where $J_1=J$. Thus this model has three independent free parameters, J_2, J_3, and one of the K_i's. It is usually desirable to develop models with few parameters so that the effects of the individual parameters are easier to identify. Explicit results presented later will be for the choice where all the K_i's are zero, $J_2=2J$, and $J_3=\frac{1}{2}J$.

III. TRANSFER-MATRIX METHOD

In this section, the transfer-matrix method is described for the present one-dimensional model. The steps taken here can be generalized without difficulty to most one-dimensional models. For this particular case, an analytic expression for the free energy is derived. Then, exact expressions for distribution, correlation, and structure functions are derived which are later solved numerically.

An exact expression for the grand canonical free energy F corresponding to the Hamiltonian in Eq. (1) is

TABLE II. The six distinct bonds in the present model.

Bond	Energy
○○	$-J_1-K_1$
○●	J_1-K_1
→○	$-J_z-K_2$
→●	J_2-K_2
→←	$-J_3-K_3$
→→	J_3-K_3

$$\exp(-\beta F)=\sum_{\{x_i\}}\exp\left[-\beta\sum_{i=1}^{N}[V_2(x_i,x_{i+1})+V_1(x_i)]\right]$$
$$=\sum_{\{x_i\}}\prod_{i=1}^{N}\exp\{-\beta[V_2(x_i,x_{i+1})+\tfrac{1}{2}V_1(x_i)+\tfrac{1}{2}V_1(x_{i+1})]\}\ , \quad (2)$$

where $\beta\equiv(k_BT)^{-1}$ is the inverse temperature. From this point on, a bar above any quantity will indicate that it has been multiplied by β. Using the bracket notation from quantum mechanics, the (a,b) matrix element of the transfer matrix is defined to be

$$\langle a|A|b\rangle\equiv\exp[-\bar{V}_2(a,b)-\tfrac{1}{2}\bar{V}_1(a)-\tfrac{1}{2}\bar{V}_1(b)]\ . \quad (3)$$

For the present model, the transfer matrix A is

$$A=\begin{bmatrix} e^{\bar{J}_1+\bar{K}_1} & e^{-\bar{J}_1+\bar{K}_1} & e^{-\bar{J}_2+\bar{K}_2+\bar{\mu}_S/2} & e^{\bar{J}_2+\bar{K}_2+\bar{\mu}_S/2} \\ e^{-\bar{J}_1+\bar{K}_1} & e^{\bar{J}_1+\bar{K}_1} & e^{\bar{J}_2+\bar{K}_2+\bar{\mu}_S/2} & e^{-\bar{J}_2+\bar{K}_2+\bar{\mu}_S/2} \\ e^{\bar{J}_2+\bar{K}_2+\bar{\mu}_S/2} & e^{-\bar{J}_2+\bar{K}_2+\bar{\mu}_S/2} & e^{-\bar{J}_3+\bar{K}_3+\bar{\mu}_S} & e^{\bar{J}_3+\bar{K}_3+\bar{\mu}_S} \\ e^{-\bar{J}_2+\bar{K}_2+\bar{\mu}_S/2} & e^{\bar{J}_2+\bar{K}_2+\bar{\mu}_S/2} & e^{\bar{J}_3+\bar{K}_3+\bar{\mu}_S} & e^{-\bar{J}_3+\bar{K}_3+\bar{\mu}_S} \end{bmatrix}\ . \quad (4)$$

Then in terms of the transfer matrix, the free energy given by Eq. (2) can be expressed as

$$\exp(-\bar{F})=\mathrm{Tr}(A^N)=\lambda_1^N+\lambda_2^N+\lambda_3^N+\lambda_4^N\ , \quad (5)$$

where the λ_i's are the eigenvalues of the transfer matrix. The eigenvalue λ_1 is defined to be the one with the largest magnitude, so that in the thermodynamic limit,

$$F=-k_BTN\ln(\lambda_1)\ . \quad (6)$$

Since the free energy must be real, λ_1 must be real and positive.

The spectral equation for the four eigenvalues is a fourth-order polynomial. However, it separates into the product of two second-order polynomials as a consequence of the spin-reversal symmetry mentioned in Sec. II. This allows us to explicitly write the eigenvalues as

$$\lambda_{1,2}=\tfrac{1}{2}(C_1+MC_3)\pm[\tfrac{1}{4}(C_1-MC_3)^2+MC_2^2]^{1/2}\ ,$$
$$\lambda_{3,4}=\tfrac{1}{2}(S_1-MS_3)\pm[\tfrac{1}{4}(S_1+MS_3)^2-MS_2^2]^{1/2}\ , \quad (7)$$

where

$$C_i\equiv e^{\bar{J}_i+\bar{K}_i}+e^{-\bar{J}_i+\bar{K}_i}\ ,$$
$$S_i\equiv e^{\bar{J}_i+\bar{K}_i}-e^{-\bar{J}_i+\bar{K}_i}\ , \quad (8)$$
$$M\equiv e^{\bar{\mu}_S}\ .$$

Calculating statistical quantities for the model usually requires the matrix elements of A^n, where n is a positive integer. In terms of the eigenvalues and eigenvectors of A, these matrix elements are

$$\langle a|A^n|b\rangle=\sum_{c=1}^{4}\langle a|\Phi|c\rangle\langle c|\Phi^{-1}|b\rangle\lambda_c^n\ , \quad (9)$$

where Φ is a matrix that contains in its i^{th} column a right eigenvector corresponding to λ_i (for $i=1$–4). Using the above results, one can now express all the statistical quantities of interest in terms of the eigenvalues and eigenvectors. The single-site probability distribution function, which gives the probability that $x_i=a$ for a particular site i, is

$$p_a=\frac{\langle a|A^N|a\rangle}{\mathrm{Tr}(A^N)}\ , \quad (10)$$

which in the thermodynamic limit becomes

$$p_a=\langle a|\Phi|1\rangle\langle 1|\Phi^{-1}|a\rangle\ . \quad (11)$$

The pair distribution function, which gives the probability that for some site i, $x_i=a$ while $x_{i+n}=b$, is given by

$$p_{ab}(n)=\frac{\langle a|A^n|b\rangle\langle b|A^{N-n}|a\rangle}{\mathrm{Tr}(A^N)}\ , \quad (12)$$

which in the thermodynamic limit can be shown to be

$$p_{ab}(n)=p_ap_b+\sum_{c=2}^{4}\Gamma_{abc}\Lambda_c^n\ , \quad (13)$$

where

$$\Gamma_{abc}\equiv\langle a|\Phi|c\rangle\langle c|\Phi^{-1}|b\rangle\langle b|\Phi|1\rangle\langle 1|\Phi^{-1}|a\rangle \quad (14)$$

and $\Lambda_c\equiv\lambda_c/\lambda_1$. Equations (12) and (13) for the pair distribution function are valid only for positive $n=0,1,2,\ldots,\infty$. Note that both these expressions give $p_{ab}(0)=p_a\delta_{ab}$. To obtain the pair distribution function for negative n, one uses $p_{ab}(-n)=p_{ba}(n)$. From the pair distribution function, one obtains the pair-correlation function,

$$c_{ab}(n)\equiv p_{ab}(n)-p_ap_b=\sum_{c=2}^{4}\Gamma_{abc}\Lambda_c^n \quad (15)$$

for $n=0,1,2,\ldots,\infty$. Similarly, for negative n one uses $c_{ab}(-n)=c_{ba}(n)$. Then from the correlation function one obtains the structure function.

$$S_{ab}(q)\equiv\sum_{n=-\infty}^{\infty}c_{ab}(n)e^{inq}$$
$$=\sum_{c=2}^{4}\left[\Gamma_{abc}\frac{\Lambda_c}{e^{-iq}-\Lambda_c}+\Gamma_{bac}\frac{\Lambda_c}{e^{iq}-\Lambda_c}\right]+\delta_{ab}p_a-p_ap_b\ . \quad (16)$$

Although it is not immediately obvious from Eq. (16), the structure function is a real valued function.

IV. RESULTS

In Fig. 1 is a contour map of the surfactant density, $\rho_S \equiv p_3 + p_4$, in the temperature-chemical-potential plane. At zero temperature, $\rho_S = 0.0$, 0.5, and 1.0 for $\mu_S < -2J$, $-2J < \mu_S < 3J$, and $\mu_S > 3J$, respectively. The two points $\mu_S = 2(J_1 + K_1 - J_2 - K_2) = -2J$ and $\mu_S = 2(J_2 + K_2 - J_3 - K_3) = 3J$ are phase transitions separating from left to right coexisting water- and oil-rich phases ($W+O$), a lamellar phase (L) and a surfactant-rich phase (S). These phases are pictured in Fig. 2. In order to have a lamellar phase, the parameters of the model must satisfy $2(J_2 + K_2) > J_1 + K_1 + J_3 + K_3$. For nonzero temperatures, there is only a single phase and consequently no phase transitions.

The eigenvalues $\lambda_{1,2}$ in Eqs. (7) are always real, but $\lambda_{3,4}$ may be complex conjugate pairs. When these eigenvalues are complex, oscillations can occur in the pair-correlation functions. Note that negative real eigenvalues may also cause oscillations, but always with a wavelength of two lattice sites. For the case examined here, λ_2 is negative and does cause such oscillations in some of the pair-correlation functions. The wavelength due to the eigenvalues $\lambda_{3,4}$ is 2π divided by the wave number $k \equiv \arg(\lambda_3)$. For small μ_S, $\lambda_{3,4}$ are positive and real so that $k = 0$, and thus $\lambda_{3,4}$ do not cause oscillations in the pair-correlation functions. As μ_S increases, the disorder line [18] (DL) is encountered where $\lambda_{3,4}$ become complex conjugate pairs, k becomes nonzero, and long-wavelength oscillations occur in some of the pair-correlation functions. As μ_s increases still more, the wavelength decreases until finally $k = \pi$ and $\lambda_{3,4}$ become real and negative. For larger μ_S, $\lambda_{3,4}$ can only cause oscillations with a wavelength of two lattice sites. In Figs. 3 and 4, lines of constant wave number are plotted, which resemble those obtained from the model in Ref. [3]. The two lines for the limiting cases, $k \to 0^+$ and $k \to \pi^-$, can be obtained analytically as they result when the terms under the square root for the second pair of eigenvalues in Eqs. (7) become zero. This occurs when

$$M = \frac{2S_2^2 - S_1S_3 \pm 2S_2(S_2^2 - S_1S_3)^{1/2}}{S_3^2}, \tag{17}$$

provided that $S_2^2 > S_1S_3$. In Eq. (17), the minus sign corresponds to the line for $k \to 0^+$ and the plus sign to the line for $k \to \pi^-$. The line for $k \to 0^+$ is in fact the DL. Figures 3 and 4 show the disorder line in the temperature-chemical-potential plane and temperature-density plane, respectively. As the temperature becomes large, Eq. (17) reduces to

$$e^{\bar{\mu}_S} \approx \frac{2J_2^2 - J_1J_3 \pm 2J_2(J_2^2 - J_1J_3)^{1/2}}{J_3^2}. \tag{18}$$

Also at high temperatures,

$$\rho_S \approx \frac{1}{1 + e^{-\bar{\mu}_S}}. \tag{19}$$

Using Eqs. (18) and (19), it follows that for the parameters selected in Sec. II, the DL approaches $\rho_S = 0.0626$ and the line for $k \to \pi-$ approaches $\rho_S = 0.9836$ as $T \to \infty$.

Figure 5 shows the resulting water-water correlation function, $c_{WW}(n) \equiv c_{11}(n)$, for various μ_S/J's at $k_BT/J = 1$. Although $c_{WW}(n)$ is a discrete function, the continuous extension of Eq. (15) has been plotted for clarity. Notice that at $\mu_S/J = -4$, $c_{WW}(n)$ is monotone decreasing, but for the higher chemical potentials in Fig. 5 $c_{WW}(n)$ oscillates. The change in the behavior of $c_{WW}(n)$

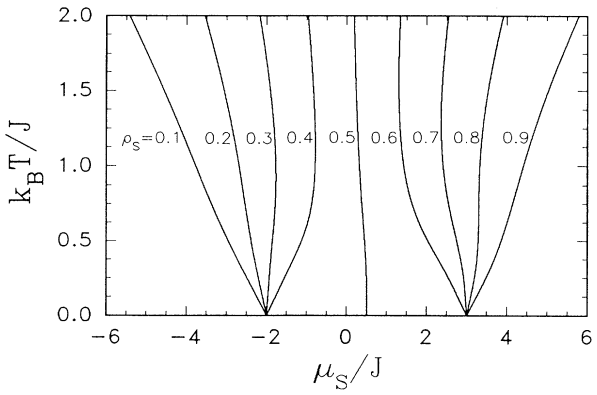

FIG. 1. A contour map of the surfactant density ρ_S in the temperature-chemical-potential plane for the parameters selected in Sec. II.

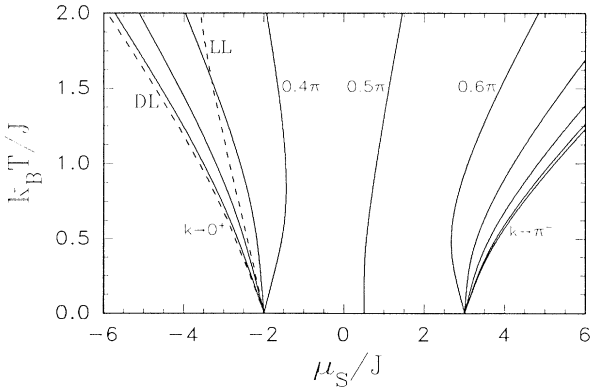

FIG. 3. A contour map of the wave number k for the long-wavelength oscillations in the water-water correlation function plotted in the temperature-chemical-potential plane. The DL and LL are shown with dashed lines.

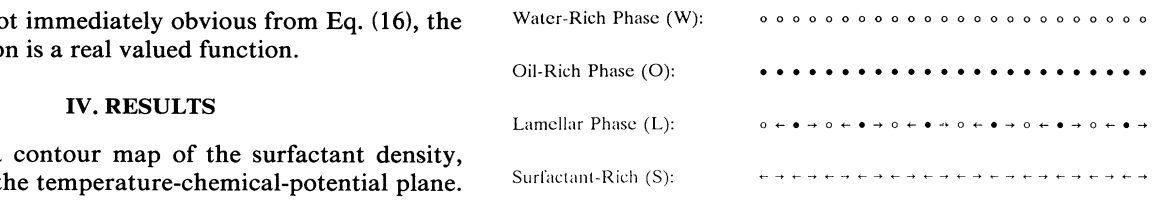

FIG. 2. Configurations of zero-temperature phases.

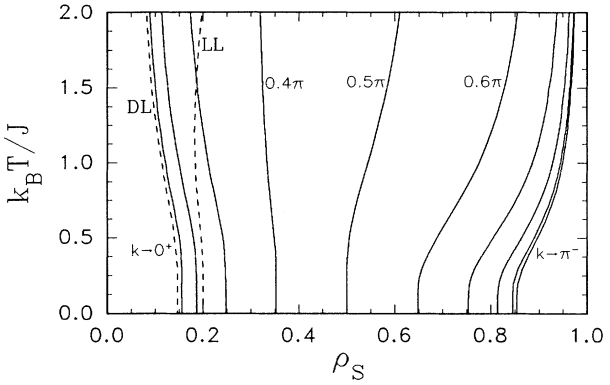

FIG. 4. The same plot as in Fig. 3, but in the temperature-density plane.

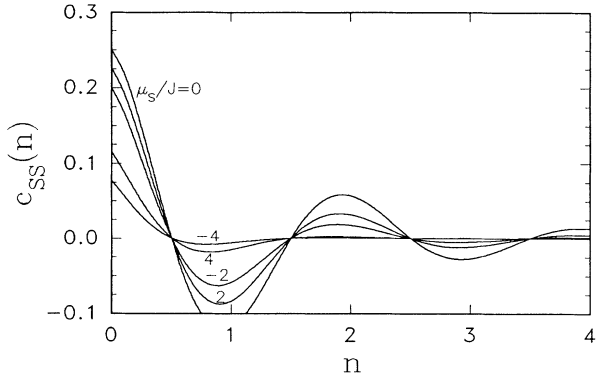

FIG. 6. The surfactant-surfactant correlation function plotted at $k_BT/J=1$ for several chemical potentials.

takes place at the DL, which at this temperature occurs at $\mu_S/J=-3.6165$. One can see in Fig. 5 that as μ_S becomes larger the wavelength of the oscillation decreases continuously. Also notice that at $\mu_S/J\sim 0$, which is in the lamellar region, the wavelength is about four lattice spacings as one should expect.

The surfactant-surfactant correlation function, $c_{SS}(n)\equiv c_{33}(n)+c_{34}(n)+c_{43}(n)+c_{44}(n)$, is plotted for several μ_S/J's at $k_BT/J=1$ in Fig. 6. In this case, the eigenvalues $\lambda_{3,4}$ do not contribute to the correlation function and thus long-wavelength oscillations do not exist in $c_{SS}(n)$. However, λ_2, which is negative in this case, causes an exponentially decaying oscillation with a fixed wavelength of two lattice spacings. Notice that the oscillations are strongest near $\mu_S/J=0$, which is natural since this is the lamellar region.

In Fig. 7 is the water-water structure function, $S_{WW}(q)\equiv S_{11}(q)$, at $k_BT/J=1$. Notice that for $\mu_S/J=-3$, the structure function only has a peak at $q=0$, but for the higher μ_S/J's in Fig. 7, the peak moves to nonzero q due to the long-wavelength oscillation in the water-water correlation function. This change in behavior of $S_{WW}(q)$ occurs at the Lifshitz line [19] (LL). To obtain the LL, $S_{WW}(q)$ is expanded in a Taylor series about $q=0$,

$$S_{WW}(q)=S_{WW}(0)+\tfrac{1}{2}S''_{WW}(0)q^2+O(q^4)\ , \tag{20}$$

where

$$S''_{WW}(0)=-2\sum_{c=2}^{4}\Gamma_{11c}\frac{(1+\Lambda_c)\Lambda_c}{(1-\Lambda_c)^3}\ . \tag{21}$$

Mathematically, the LL corresponds to the solution of $S''_{WW}(0)=0$. The LL is plotted in the temperature-surfactant-chemical-potential plane in Fig. 3 and in the temperature-surfactant-density plane in Fig. 4. One can also see a pronounced peak in $S_{WW}(q)$ at $q=\pi$, which is a signature of the lamellar region. In Fig. 8 are similar plots for $S_{SS}(q)\equiv S_{33}(q)+S_{34}(q)+S_{43}(q)+S_{44}(q)$. They are rather simple, only having a peak at $q=\pi$, which is strongest near $\mu_S/J=0$ where the lamellar region exists.

Unlike the DL, the LL does not extend to infinite temperature, but instead bends to the right, terminating at a finite temperature and $\rho_S=1$. To calculate the temperature where the LL terminates, one must solve for Φ and Φ^{-1} to order $M^{-1/2}$. These matrices are not unique, but any one of the possible solutions will do, such as

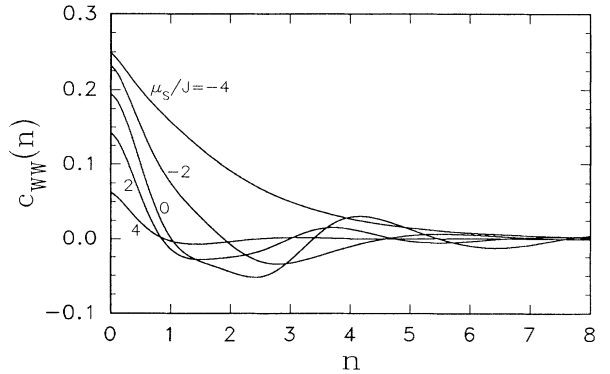

FIG. 5. The water-water correlation function plotted at $k_BT/J=1$ for several chemical potentials.

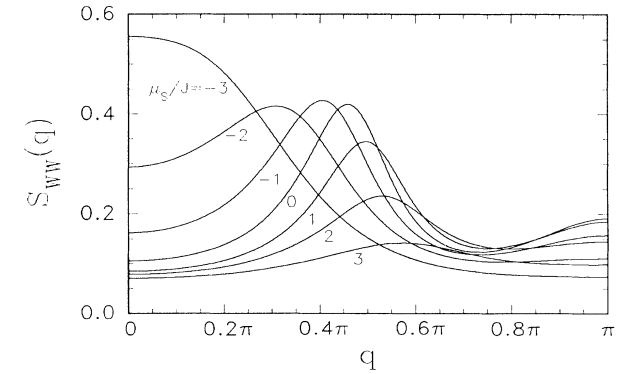

FIG. 7. The water-water structure function plotted at $k_BT/J=1$ for several chemical potentials.

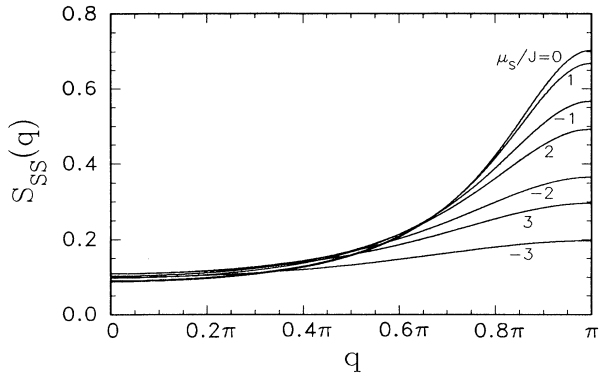

FIG. 8. The surfactant-surfactant structure function plotted at $k_BT/J=1$ for several chemical potentials.

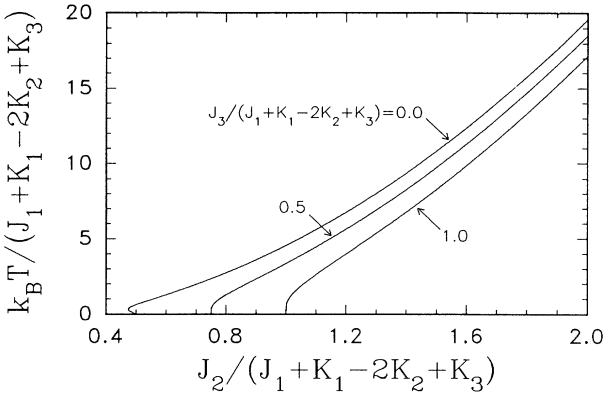

FIG. 9. The temperature at which the Lifshitz line intercepts the $\rho_s=1$ line for various values of the parameters.

$$\Phi\approx\frac{1}{\sqrt{2}}\begin{bmatrix}(C_2/C_3)M^{-1/2} & 1 & 1 & (S_2/S_3)M^{-1/2}\\ (C_2/C_3)M^{-1/2} & 1 & -1 & -(S_2/S_3)M^{-1/2}\\ 1 & -(C_2/C_3)M^{-1/2} & (S_2/S_3)M^{-1/2} & 1\\ 1 & -(C_2/C_3)M^{-1/2} & -(S_2/S_3)M^{-1/2} & -1\end{bmatrix} \tag{22}$$

and

$$\Phi^{-1}\approx\frac{1}{\sqrt{2}}\begin{bmatrix}(C_2/C_3)M^{-1/2} & (C_2/C_3)M^{-1/2} & 1 & 1\\ 1 & 1 & -(C_2/C_3)M^{-1/2} & -(C_2/C_3)M^{-1/2}\\ 1 & -1 & -(S_2/S_3)M^{-1/2} & (S_2/S_3)M^{-1/2}\\ -(S_2/S_3)M^{-1/2} & (S_2/S_3)M^{-1/2} & 1 & -1\end{bmatrix}. \tag{23}$$

From these matrices, the values of the Γ_{11c}'s can be calculated for large M or $\rho_S\approx 1$. Also for large M, the eigenvalues given by Eqs. (7) are

$$\begin{aligned}\lambda_1&\approx C_3M\ ,\\ \lambda_2&\approx\frac{C_1C_3-C_2^2}{C_3}\ ,\\ \lambda_3&\approx\frac{S_1S_3-S_2^2}{S_3}\ ,\\ \lambda_4&\approx -S_3M\ .\end{aligned} \tag{24}$$

From Eqs. (24), one obtains the Λ_c's for large M. Substituting these results into Eq. (21) and equating it to zero gives the condition that must be satisfied by the LL as $M\to\infty$ or $\rho_S\to 1$, which is

$$\frac{\sinh^2(\bar{J}_2)}{\sinh(\bar{J}_3)}\left[\frac{1-\tanh(\bar{J}_3)}{[1+\tanh(\bar{J}_3)]^3}-1\right]-\frac{\cosh^2(\bar{J}_2)}{\cosh(\bar{J}_3)}+\exp(\bar{J}_1+\bar{K}_1-2\bar{K}_2+\bar{K}_3)=0\ . \tag{25}$$

For the parameters selected, the solution to Eq. (25) and thus the temperature at which the LL terminates is $k_BT/J=18.5057$. For other parameters, the temperature at which the LL intercepts the $\rho_s=1$ line is plotted in Fig. 9. From this figure, it is clear that J_2, which controls the amphiphilic strength of the surfactant, has much more effect on the upper temperature limit of the LL than J_3. If J_2 becomes less than $\frac{1}{2}(J_1+J_3+K_1-2K_2+K_3)$ so that the zero-temperature lamellar phase does not exist, then LL usually does not exist. An exception occurs when J_2 is nearly large enough to produce the lamellar phase and J_3 is close to zero, in which case the LL begins from the $\rho_S=1$ line at a nonzero temperature rather than from $\rho_S<1$ and zero temperature. In this case, the LL intercepts the $\rho_s=1$ line twice, which is what causes the line for $J_3=0$ in Fig. 9 to become double valued for small J_2.

V. DISCUSSION

The most notable limitation of this one-dimensional model is the lack of phase transitions. As mentioned earlier, there are only phase transitions at zero temperature between the $W+O$ and L phases, and between the L and S phases. When this model is considered on higher-dimensional lattices [2], these phase transitions extend upward to nonzero temperatures forming first-order lines separating the different phases. Eventually as tempera-

ture increases, the $W+O$, L, and S phases usually terminate at first-order transitions with a disordered phase (D). For low surfactant concentrations, the transition between $W+O$ and D is second order.

At zero temperature where the phase transitions occur, at $\mu_S/J=-2$ and 3 in the present case, the system is completely degenerate. There is an infinite number of ground states at each of these two points (sometimes referred to as "frustration points" [20]). In Ref. [3], there is a similar point between the $W+O$ and L phases, which is considered more extensively. Such points also exist on higher-dimensional lattices. In fact, the present model on higher-dimensional lattices can exhibit various longer-period lamellar phases which exist in very narrow regions extending upward from these degeneracy points.

Although there is only one phase at nonzero temperature, characteristics of each zero-temperature phase persist over a range of chemical potential at low temperatures. For example, the model will exhibit characteristics of the lamellar phase at low temperatures and $\mu_S/J\approx 0$, since for the parameters selected this is above the zero-temperature lamellar phase. In this lamellarlike region, there is a tendency to have sequential sites occupied by water, surfactant, oil, surfactant, water, and so on, where the surfactant molecules tend to point towards sites occupied by water. Consequently, $\rho_S\approx 0.5$, the water-water correlation function has an oscillation with a wavelength of about four lattice sites, the water-water structure function has a peak at about $q\approx 0.5\pi$, the surfactant-surfactant correlation function has an oscillation with a wavelength equal to two lattice sites, and the surfactant-surfactant structure function has a strong peak at $q=\pi$. For low temperature and low chemical potential, the nonzero temperature phase behaves like the zero-temperature $W+O$ phases. In this region, ρ_S is small and the water-water correlation length is long. Similarly, for low temperature and high chemical potential, there is a surfactant-rich region where sites are predominantly occupied by surfactant molecules with orientation alternating from site to site.

At high temperatures, the single phase for this one-dimensional model behaves similarly to the disordered phase (D) which exists on higher-dimensional lattices. This phase is of interest because it is thought to contain the microemulsion region along with a region of ordinary disordered fluid [1–7]. The line which separates the D phase into these two regions is not a phase boundary and is not clearly defined. The DL and the LL introduced in Sec. IV are the two common choices for this dividing line [3–5,21]. The region to the side of the dividing line with higher surfactant concentration is considered to be the microemulsion region. The DL is perhaps the more realistic dividing line, since the structure of the microemulsion is thought to cause the oscillation in the water-water correlation function. However, the more practical function to measure is the structure function, obtained by scattering experiments. Thus the LL is experimentally easier to determine than the DL.

This one-dimensional model is about the simplest possible model which produces correlation functions, structure functions, and disorder lines with what we believe is the correct behavior for the disordered phase of water-oil-surfactant mixtures. This behavior can be summarized by describing what happens as μ_S and thus ρ_S are increased while the temperature is held fixed. For small ρ_S, there is ordinary disordered fluid where the water-water correlation function decreases monotonously and the water-water structure function has its maximum at $q=0$. As ρ_s is increased, the DL is encountered and the water-water correlation function develops very long-wavelength oscillations signifying the microemulsion region. When ρ_S increases still farther, the oscillation in the correlation function becomes stronger and the wavelength decreases, finally producing a peak in the water-water structure function at small nonzero q. The more ρ_S increases and one moves deeper into the microemulsion region, the wavelength of the oscillation in the correlation function decreases and the peak in the structure function moves to larger q. Note that the LL occurs at higher surfactant concentration than the DL since the long-wavelength oscillations must be present before the peak in the water-water structure function will move to nonzero q. The surfactant-surfactant correlation function never develops the long-wavelength oscillation and thus the surfactant-surfactant structure function never develops a peak at small nonzero q, which is in agreement with experiment. Other structure functions can be obtained from the two given and using identities such as $S_{WS}(q)=-\frac{1}{2}S_{SS}(q)$ and $S_{WO}(q)=-S_{WW}(q)-S_{WS}(q)$ [4].

It is the tendency for surfactant molecules to locate themselves at water-oil interfaces which is supposedly responsible for microemulsions. Thus it is not surprising that J_2 and K_2 are important for the existence of the microemulsion region. This is because in order to produce the long-wavelength oscillation in the water-water correlation function, the transfer matrix must have complex eigenvalues. This is not possible if $J_2=0$ because then the transfer matrix Eq. (4) is symmetric and thus only produces real eigenvalues. However, once $J_2>0$, the symmetry of the transfer matrix is broken. These symmetry-breaking terms become larger for larger J_2 and K_2, favoring complex eigenvalues as can be seen from Eqs. (7). This is true also on the two- and three-dimensional lattices.

The locations of the disorder line and the Lifshitz line differ substantially at high temperatures. This is consistent with the behavior of these two lines on higher-dimensional lattices for the present model [2,22]. The DL always seems to approach an asymptotic surfactant density as $T\rightarrow\infty$ as it did in the present one-dimensional case. As for the LL, approximations for higher-dimensional lattices seem to agree that it terminates at a finite temperature with $\rho_S=1$ [2]. Results for the model in Refs. [3–5] predict that the Lifshitz line extends to infinite temperature. The reason this happens is that the amphiphilic interactions in those references are associated with a temperature-independent three-particle potential. In practice, such interactions should decrease with temperature due to entropic effects associated with the underlying orientational degrees of freedom [10,23]. If this were done, there would be a finite temperature where

the amphiphilic interaction becomes too small to produce a microemulsion. When this is taken into account in a similar model of binary water-surfactant mixtures [15], a LL is found which appears to terminate at a finite temperature.

ACKNOWLEDGMENT

This work has been supported by a grant from the Natural Sciences and Engineering Research Council, Canada.

[1] K. Chen, C. Ebner, C. Jayaprakash, and R. Pandit, Phys. Rev. A **38**, 6240 (1988).
[2] M. W. Matsen and D. E. Sullivan, Phys. Rev. A **41**, 2021 (1990).
[3] G. Gompper and M. Schick, Phys. Rev. A **42**, 2137 (1990).
[4] G. Gompper and M. Schick, Phys. Rev. B **41**, 9148 (1990).
[5] G. Gompper and M. Schick, Phys. Rev. Lett. **62**, 1647 (1989).
[6] A. Ciach, J. Chem. Phys. **93**, 5322 (1990).
[7] B. Widom, J. Chem. Phys. **90**, 2437 (1989).
[8] B. Widom, J. Chem. Phys. **84**, 6943 (1986); K. A. Dawson, Phys. Rev. A **36**, 3383 (1987); K. A. Dawson, M. D. Lipkin, and B. Widom, J. Chem. Phys. **88**, 5159 (1988); K. A. Dawson, B. L. Walker, and A. Bereva, Physica A **165**, 320 (1990).
[9] G. Gompper and M. Schick, in *Modern Ideas and Problems in Amphiphilic Science,* edited by W. M. Gelbart, D. Roux, and A. Ben-Shaul (Springer-Verlag, Berlin, in press).
[10] G. M. Carneiro and M. Schick, J. Chem. Phys. **89**, 4368 (1988).
[11] M. Schick and W. H. Shih, Phys. Rev. Lett. **59**, 1205 (1987).
[12] A. Ciach, J. S. Høye and G. Stell, J. Phys. A **21**, L777 (1988); J. Chem. Phys. **90**, 1214 (1989); A. Ciach and J. S. Høye, *ibid.* **90**, 1222 (1989).
[13] M. M. Telo da Gama and K. E. Gubbins, Mol. Phys. **59**, 227 (1986).
[14] M. Schick and W. H. Shih, Phys. Rev. B **35**, 1797 (1986).
[15] G. Gompper and M. Schick, Chem. Phys. Lett. **163**, 475 (1989).
[16] J. W. Halley and A. J. Kolan, J. Chem. Phys. **88**, 3313 (1988); J. R. Gunn and K. A. Dawson, *ibid.* **91**, 6393 (1989); K. A. Dawson and Z. Kurtovic, *ibid.* **92**, 5473 (1990).
[17] V. Z. S. Shante and S. Kirkpatrick, Adv. Phys. **20**, 325 (1971).
[18] J. Stephenson, J. Math. Phys. **11**, 420 (1970).
[19] R. M. Hornreich, R. Liebmann, H. G. Schuster, and W. Selke, Z. Phys. B **35**, 91 (1979).
[20] R. Liebmann, *Statistical Mechanics of Periodic Frustrated Ising Systems,* Lecture Notes in Physics Vol. 251 (Springer-Verlag, Berlin 1986).
[21] In earlier publications, the line now referred to as the Lifshitz line often went unnamed or as in Refs. [5] and [6] was called a disorder line.
[22] Our results showing the behavior of the disorder line in two and three dimensions and the Lifshitz line in two dimensions are as yet unpublished.
[23] C. A. Vause and J. S. Walker, Phys. Lett. **90A**, 419 (1982).